Preprints of the 21st IFAC World Congress (Virtual)
Berlin, Germany, July 12-17, 2020

Extended Fractional-Order Memory Reset Control for Integer-Order LTI Systems and Experimental Demonstration

Christoph Weise, Kai Wulff, Johann Reger ⋆

Control Engineering Group, Technische Universität Ilmenau, 98684, Ilmenau, Germany

Abstract: In this work we extend the concept of fractional-order memory reset control. A fractional-order controller is applied to an integer-order plant and its memory is deleted periodically. As an extension, the controller state itself is reset, based on the reference and the error signal. The closed loop can be represented by a fractional-order hybrid system with induced discrete dynamics. These are used to tune the reset law and to prove exponential stability. By means of the extended reset strategy the reset intervals can be reduced, such that less memory is needed to implement the fractional-order operators. Furthermore, a new approach for the real-time implementation of memory reset controllers is presented that achieves a decrease of the numerical error. All results are validated by simulations and experimentally.

1. INTRODUCTION

During the last decades, controllers containing non-integer derivatives, so-called fractional-order (FO) controllers, gained increasing attention. Especially the simple expansion of the classical PID controller to arbitrary order features more degrees of freedom for loop-shaping tasks (Monje et al., 2010). However, linear FO controllers show two main disadvantages: First, the implementation requires a lot of physical memory (Monje et al., 2010) and can only use a partial history of the process. Second, the algebraic convergence of the FO closed-loop system is slow compared to the exponential decay rate of integer-order systems. In order to overcome these drawbacks, a memory-reset of the controller is proposed by Weise et al. (2019) to achieve also exponential convergence.

A different approach is taken by HosseinNia et al. (2014b), where a FO reset controller is proposed to improve integer-order reset controllers by reducing limit cycles to increase the performances with respect to the set-point regulation problem (HosseinNia et al., 2013). Although these two approaches deal with the reset of FO controllers, they lead to completely different results. The main objective of this contribution is a comparison of these methods. Furthermore we extend the concept of memory reset control and introduce a numerical method that is suitable to be implemented in real-time.

This paper is organized as follows: In Section 2 we recall fundamentals properties of FO-LTI systems defined by Caputo's operator. In the following parts we revisit two FO reset controllers that reset periodically. The first controller by HosseinNia et al. (2014b) works with an explicit state reset, whereas the second controller by Weise et al. (2019) only deletes the memory without resetting the controller state. In Section 3 we combine both approaches, provide sufficient stability conditions and use the frequency domain interpretation to tune the reset law. Section 4 details on the implementation of all shown controllers using higher-order approximations and a direct approach to solve the FO integral. The performance of the presented controller is evaluated experimentally in Section 5. Conclusions are drawn in Section 6.

⋆ Corresponding author: johann.reger@tu-ilmenau.de

2. PRELIMINARY RESULTS AND DEFINITIONS

2.1 Fractional-Order Operators

Non-integer-order derivatives combine classical integer-order derivatives with the FO integral. This is given by Monje et al. (2010); Podlubny (1999) as per

$$ {}_{t_0}\mathcal{I}^{\alpha} f(t) = \frac{1}{\Gamma(\alpha)} \int_{t_0}^{t} (t-\tau)^{\alpha-1} f(\tau) \mathrm{d}\tau, \quad t > t_0, \tag{1} $$

with the order of integration $\alpha \in \mathbb{R}^+$ and Euler's Gamma function $\Gamma(\cdot)$. The integral is a convolution of the function $f(\cdot)$ with the convolution kernel $Y_\alpha(\cdot)$ defined in Matignon (1996):

$$ Y_\alpha(t) = \frac{(t-t_0)_+^{\alpha-1}}{\Gamma(\alpha)} \in L^1_{\mathrm{loc}}(\mathbb{R}^+). \tag{2} $$

The combination with classical integer-order derivatives leads to the definition of different FO derivatives. In this contribution we will apply Caputo's operator defined by

$$ {}_{t_0}\mathcal{D}^{\alpha}_{t} f(t) = \frac{1}{\Gamma(m-\alpha)} \int_{t_0}^{t} \frac{f^{(m)}(\tau)}{(t-\tau)^{\alpha-m+1}} \mathrm{d}\tau, \tag{3} $$

where $\alpha \in \mathbb{R}^+$ is the order of differentiation and m is an integer such that $m-1 \leq \alpha < m$. We are considering the control of integer-order systems, hence this operator seems more suitable due to a similar interpretation of the initial conditions and available numerical tools. As per Monje et al. (2010) the Laplace-transform of the operator is

$$\mathcal{L}\{{}_0\mathcal{D}_t^\alpha f(t)\} = s^\alpha \mathcal{L}\{f(t)\} - \sum_{k=0}^{m-1} s^{\alpha-k-1} f^{(k)}(0^+). \quad (4)$$

Due to the contained FO integral within the definition, Caputo's derivative is a non-local operator and has memory. Therefore we have in general

$${}_{t_1}\mathcal{D}^\alpha f(t) \neq {}_{t_2}\mathcal{D}^\alpha f(t), \quad \alpha \notin \{\mathbb{N}, 0\}. \quad (5)$$

2.2 Fractional-Order LTI System

The FO-LTI system with (classical) initial conditions $x(t_0) = x_0$ is given by:

$$\Sigma : \begin{cases} {}_{t_0}\mathcal{D}^\alpha x(t) = Ax(t) + Bu(t) & \text{(6a)} \\ y(t) = Cx(t) + Du(t) & \text{(6b)} \end{cases}$$

with (pseudo) state $x(t) \in \mathbb{R}^n$, input $u(t) \in \mathbb{R}^p$, output $y(t) \in \mathbb{R}^q$, order of differentiation $\alpha \in (0, 2)$ and matrices $A \in \mathbb{R}^{n\times n}$, $B \in \mathbb{R}^{n\times p}$, $C \in \mathbb{R}^{q\times n}$ and $D \in \mathbb{R}^{q\times p}$.

For the case of $\alpha > 1$ the set of initial conditions is not sufficient to guarantee uniqueness of the solution. Additional initial conditions are required, see (4). With the representation of (6) these are set to zero, i.e. $\dot{x}(t_0) = 0$.

Compared to integer-order systems the pseudo transition-matrix in the FO case is defined by the Matrix-Mittag-Leffler function

$$\mathcal{E}_{\alpha,\beta}\left(A(t-t_0)^\alpha\right) = \sum_{k=0}^{\infty} \frac{(A(t-t_0)^\alpha)^k}{\Gamma(\alpha k + \beta)} \quad (7)$$

with $\alpha, \beta > 0$. Applying this transition matrix solves the initial value problem (Monje et al., 2010; Podlubny, 1999):

$$x(t) = \mathcal{E}_{\alpha,1}(At^\alpha)x_0 + \int_0^t \tau^{\alpha-1}\mathcal{E}_{\alpha,\alpha}(A\tau^\alpha)Bu(t-\tau)\mathrm{d}\tau. \quad (8)$$

Theorem 1. (FO-LTI System Stability (Matignon, 1996)). The origin of the system Σ is asymptotically stable iff

$$|\arg(\lambda_i(A))| > \alpha\frac{\pi}{2}, \quad \forall i = 1, 2, \ldots, n, \quad (9)$$

where $\lambda_i(A)$ denotes the i-th eigenvalue of A.

Note that asymptotically stable FO systems with $\alpha < 1$ may exhibit eigenvalues with positive real part.

If some FO-LTI controller is applied to an integer-order LTI system it is useful to represent the closed-loop with unified order of operation. Although FO systems may be represented by time-varying integer-order systems (Weise et al., 2016), it is simpler to express the integer-order process by using FO derivatives.

Any FO system with order α may also be expressed using a different order of differentiation $\bar{\alpha} = \frac{\alpha}{\kappa}$ with $\kappa \in \mathbb{N}$. The state of this associated FO system is extended with additional FO derivatives (Weise et al., 2019) or integrals (Weise et al., 2017) of the original (pseudo) state, i.e.

$$\bar{x}(t) = \left(x^\top(t)\ {}_{t_0}\mathcal{D}^\alpha x^\top(t)\ \cdots\ {}_{t_0}\mathcal{D}^{(\kappa-1)\alpha}x^\top(t)\right)^\top. \quad (10)$$

The FO dynamics with respect to the order $\bar{\alpha}$ finally read

$${}_{t_0}\mathcal{D}^{\bar{\alpha}}\bar{x}(t) = \underbrace{\begin{pmatrix} 0 & I_{n(\kappa-1)\times n(\kappa-1)} \\ A & 0 \end{pmatrix}}_{\bar{A}\in\mathbb{R}^{\kappa n\times\kappa n}}\bar{x}(t) + \underbrace{\begin{pmatrix} 0 \\ B \end{pmatrix}}_{\bar{B}\in\mathbb{R}^{\kappa n\times p}}u(t) \quad (11)$$

and correspond to the initial condition

$$\bar{x}(t_0) = \left(x_0^\top\ 0\ \cdots\ 0\right)^\top. \quad (12)$$

The output for this extended state $\bar{x}(t)$ is given by

$$y(t) = (C\ 0\ \cdots\ 0)\,\bar{x}(t) + Du(t) = \bar{C}\bar{x}(t) + \bar{D}u(t). \quad (13)$$

The construction of this associated system follows the ideas presented by Weise et al. (2017). The Laplace-transform is applied to (11) for each block, defining the extended state ${}_{t_0}\mathcal{D}^{i\alpha}x(t)$ with $i = 0, 1, \ldots, \kappa-1$. Setting the initial condition of the auxiliary states to zero (see (12)) we can solve this system of κ matrix equations resulting in the Laplace-transform of (6a). Hence, output trajectories of both systems are identical such that

$$G(s) = C(s^\alpha I - A)^{-1}B + D = \bar{C}(s^{\bar{\alpha}}I - \bar{A})^{-1}\bar{B} + \bar{D}.$$

2.3 Fractional-Order State Reset Control

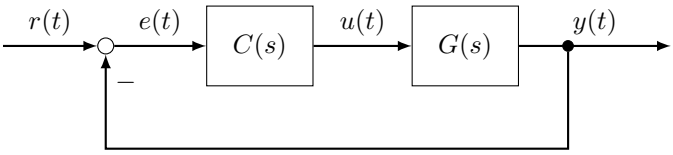

Fig. 1. Block diagram of a reset control scheme without disturbances.

Reset controllers are used to enhance the performance of linear control systems. There are various approaches targeting different kinds of problems, e.g. controllers resetting their state based on the error signal (when $e(t) = 0$) are designed in order to avoid overshooting (HosseinNia et al., 2014b,a) whereas the reset strategy of predetermined resetting times (periodic resetting) is applied to accelerate the closed-loop system (Zheng et al., 2008).

We consider the standard output feedback loop depicted in Fig. 1. In (HosseinNia et al., 2014b, 2013) the idea of a periodically reset integer-order controller was expanded to the FO description

$$\begin{aligned} {}_{t_0}\mathcal{D}^\alpha x_\mathrm{c}(t) &= A_\mathrm{c}x_\mathrm{c}(t) + B_\mathrm{c}e(t), & t \neq t_k & \quad \text{(14a)} \\ x_\mathrm{c}(t_k^+) &= M_\mathrm{c}x_\mathrm{c}(t_k) + N_\mathrm{c}r(t_k) + P_\mathrm{c}e(t_k), & t = t_k & \quad \text{(14b)} \\ u(t) &= C_\mathrm{c}x_\mathrm{c}(t) + D_\mathrm{c}e(t) & & \quad \text{(14c)} \end{aligned}$$

with $x_\mathrm{c}(t) \in \mathbb{R}^\eta$ and constant reset period $\delta = t_{k+1} - t_k$, $k = 0, 1, \ldots$. This controller consist of an underlying baseline controller defined by (14a) and (14c), that is, $C(s) = C_\mathrm{c}(s^\alpha I - A_\mathrm{c})^{-1}B_\mathrm{c} + D_\mathrm{c}$ and is extended by the reset equation (14b). This reset law is a generalization of the reset presented by HosseinNia (2013); HosseinNia et al. (2014a): At each time instant t_k the controller state is reset, based on the current controller state $x_\mathrm{c}(t_k)$, the reference signal $r(t_k)$ and the error signal $e(t_k) = r(t_k) - y(t_k)$. Note that this reset law only requires output measurements, whereas the reset law shown by Zheng et al. (2008) uses the process state as well.

We consider the integer-order system (6) with $\alpha = 1$ and apply the FO reset controller (14) with $\bar{\alpha}^{-1} \in \mathbb{N}$. The closed loop dynamics combing the extended process state $\bar{x}$ and the controller state x_c to $z^\top := \left(\bar{x}^\top\ x_\mathrm{c}^\top\right)^\top$ without the reset $t \neq t_k$ are

$$ {}_{t_0}\mathcal{D}^{\alpha} z(t) = \underbrace{\begin{pmatrix} \bar{A} - \bar{B}D_{\mathrm{c}}\bar{C} & \bar{B}C_{\mathrm{c}} \\ -B_{\mathrm{c}}\bar{C} & A_{\mathrm{c}} \end{pmatrix}}_{=:F} z(t) + \underbrace{\begin{pmatrix} \bar{B}D_{\mathrm{c}} \\ B_{\mathrm{c}} \end{pmatrix}}_{=:B_{\mathrm{cl}}} r(t) \quad (15a) $$

$$ y(t) = \underbrace{\begin{pmatrix} \bar{C} - \bar{D}D_{\mathrm{c}}\bar{C} & \bar{D}C_{\mathrm{c}} \end{pmatrix}}_{=:C_{\mathrm{cl}}} z(t) + \underbrace{\begin{pmatrix} \bar{D}D_{\mathrm{c}} \end{pmatrix}}_{=:D_{\mathrm{cl}}} r(t). \quad (15b) $$

At the reset instants $t = t_k$ the closed loop dynamics are reduced to the reset equation

$$ z(t_k^+) = \begin{pmatrix} I_{n\kappa \times n\kappa} & 0 \\ -\bar{C}P_{\mathrm{c}} & M_{\mathrm{c}} \end{pmatrix} z(t_k) + \begin{pmatrix} 0 \\ N_{\mathrm{c}} + P_{\mathrm{c}} \end{pmatrix} r(t_k). \quad (16) $$

Note that the extended states of $\bar{x}(t_k)$ remain unchanged due to the choice of the operator ${}_{t_0}\mathcal{D}^{\alpha}$ starting at the initial time t_0. Hence, the memory of the operator stays the same.

The stability assessment of this closed loop dynamics is not straightforward. In (HosseinNia et al., 2013) the stability was assessed using the so-called H_β-condition. The basic idea here is motivated by linear integer-order hybrid systems. For this system class a common quadratic Lyapunov function is used to guarantee the stability within one time interval and at the reset instant. The positive definite matrix P hence has to satisfy a continuous and a discrete Lyapunov inequality. For FO hybrid systems the linear matrix inequality (LMI) assuring the stability within one interval is replaced by an adopted LMI assuring the stability of the linear FO continuous time dynamics (Sabatier et al., 2010). Note that these FO-LMI conditions are not associated to a Lyapunov function.

Compared to integer-order reset control and FO memory reset control we cannot derive an exact description of the induced discrete dynamics, even though the reset interval is constant $\delta = t_{k+1} - t_k$. A pragmatic approach is to investigate the higher order integer-order approximation of the closed loop dynamics (see Section 4.1) which may be used for the implementation of such controllers.

2.4 Fractional-Order Memory Reset Control

The concept of FO memory reset control is slightly different. The idea is to reset not the state, but the memory of the FO operator to zero. A periodic memory-reset controller with $x_{\mathrm{c}}(t) \in \mathbb{R}^{\eta}$, $t_k = \delta k$ and $\alpha^{-1} \in \mathbb{N}$ is given by Weise et al. (2019) as per

$$ {}_{k\delta}\mathcal{D}^{\alpha} x_{\mathrm{c}}(t) = A_{\mathrm{c}}x_{\mathrm{c}}(t) + B_{\mathrm{c}}e(t), \quad t \in [k\delta, (k+1)\delta) \quad (17a) $$

$$ x_{\mathrm{c}}(t_k) = x_{\mathrm{c}}(t_k^-), \quad t = k\delta \quad (17b) $$

$$ u(t) = C_{\mathrm{c}}x_{\mathrm{c}}(t) + D_{\mathrm{c}}e(t) \quad (17c) $$

where the reset equation (17b) does not affect the controller states. The control signal is continuous but not differentiable due to the changing initialization of the FO integrator.

Regarding the closed loop dynamics we have to partially reset the extended states $\bar{x}$ of the integer-order process now, due to the change of the operator's initial time. This is possible because the plant to be controlled is integer-order and time invariant, hence

$$ {}_{t_1}\mathcal{D}^{1} x(t) = {}_{t_2}\mathcal{D}^{1} x(t). \quad (18) $$

The closed loop dynamics are identical except for the time varying operator and changed reset equation:

$$ z(t_k) = \begin{pmatrix} I_{n\times n} & 0 & 0 \\ 0 & 0_{n(\kappa-1)\times n(\kappa-1)} & 0 \\ 0 & 0 & I_{\eta} \end{pmatrix} z(t_k^-) = M z(t_k^-). \quad (19) $$

With this controller we can apply (8) to the closed loop system on each interval and derive an explicit description of the induced discrete dynamics for $r(t) = 0$:

$$ z(k\delta) = M\mathcal{E}_{\bar{\alpha},1}\left(F\delta^{\bar{\alpha}}\right) z((k-1)\delta) = A_{\mathrm{d}} z((k-1)\delta). \quad (20) $$

Such induced discrete-time system can be used to assess the stability of the closed loop system as shown by Zheng et al. (2008); Weise et al. (2019), evaluating the eigenvalues of A_{d} with respect to the unit circle. The periodic reset of the memory leads to the exponential convergence of the state and also allows to use unstable baseline controllers since the stability of the non-reset FO system is not necessary (Weise et al., 2019). These unstable modes may accelerate the controller response (Nesić et al., 2011).

3. CONTROLLER DESIGN

With the memory reset scheme by Weise et al. (2019) exponential convergence of the closed loop system is achieved. Smaller reset intervals result in faster convergence and less memory usage. However, this results in frequency peaks around the crossover frequency (e.g. see Fig. 3) causing large overshoots in the step response and even unstable behavior. In the following we present a control design combining memory and state reset to overcome these limitations.

3.1 Extended Fractional-Order Memory Reset Control

An extended FO memory reset controller with $x_{\mathrm{c}}(t) \in \mathbb{R}^{\eta}$ and $\alpha^{-1} \in \mathbb{N}$ is given for $k = 0, 1, \ldots$ by

$$ {}_{k\delta}\mathcal{D}^{\alpha} x_{\mathrm{c}}(t) = A_{\mathrm{c}}x_{\mathrm{c}}(t) + B_{\mathrm{c}}e(t), \quad t \in [k\delta, (k+1)\delta) \quad (21a) $$

$$ x_{\mathrm{c}}(k\delta) = M_{\mathrm{c}}x_{\mathrm{c}}(k\delta^-) + N_{\mathrm{c}}r(k\delta^-) + P_{\mathrm{c}}e(k\delta^-), \quad t = k\delta \quad (21b) $$

$$ u(t) = C_{\mathrm{c}}x_{\mathrm{c}}(t) + D_{\mathrm{c}}e(t). \quad (21c) $$

With the same baseline controller this leads to similar closed-loop dynamics (15) as in the previous section. Only the reset law changes to

$$ {}_{k\delta}\mathcal{D}^{\alpha} z(t) = Fz(t) + B_{\mathrm{cl}}r(t), \quad t \in [k\delta, (k+1)\delta) \quad (22a) $$

$$ z(k\delta) = \bar{M}z(k\delta^-) + \bar{P}r(k\delta), \quad t = k\delta \quad (22b) $$

$$ y(t) = C_{\mathrm{cl}}z(t) + D_{\mathrm{cl}}r(t) \quad (22c) $$

with the update matrices

$$ \bar{M} = \begin{pmatrix} I_{n\times n} & 0 & 0 \\ 0 & 0_{n(\kappa-1)\times n(\kappa-1)} & 0 \\ -P_{\mathrm{c}}C & 0 & M_{\mathrm{c}} \end{pmatrix}, \bar{P} = \begin{pmatrix} 0 \\ 0 \\ N_{\mathrm{c}} + P_{\mathrm{c}} \end{pmatrix}. \quad (23) $$

Similar to the pure memory reset control scheme we can reduce the stability analysis to the evaluation of the induced discrete dynamics.

Theorem 2. (Stability). The origin of the closed-loop (22) is asymptotically stable if and only if

$$ \left|\lambda_i\left(\bar{M}\mathcal{E}_{\alpha,1}\left(F\delta^{\alpha}\right)\right)\right| < 1, \quad (24) $$

for all $i = 1, 2, \ldots, \kappa n + \eta$, where $\lambda_i(\cdot)$ denotes the i-th eigenvalue of the induced discrete system matrix.

Proof. The proof follows the ideas presented in (Zheng et al., 2008; Weise et al., 2019). Since the linear FO system has no finite escape time we can reduce the stability analysis to the reset instants. The sequence of the extended states $(z(k\delta))$ for $k = 0, 1, \dots$ is defined by the induced discrete dynamics

$$z(k+1) = A_\mathrm{d} z(k) \tag{25}$$

where system matrix A_d is given by the projection of the pseudo transition matrix in (8) as per

$$A_\mathrm{d} = \bar{M}\mathcal{E}_{\alpha,1}(F\delta^\alpha). \tag{26}$$

Finally the stability of (25) can be assessed by standard methods, e.g. see (Rugh, 1996).

Note that an extension of this idea to control FO processes is not straightforward. We cannot delete the memory of the physical system and a change of the operators initial time would introduce additional time-varying inputs, the so called initialization functions (Lorenzo and Hartley, 2001). These initialization functions decay, however have to be taken into account for the stability analysis.

The induced discrete time system can also be used to give an approximation of the frequency response of the closed loop system for frequencies below the reset frequency $\omega < \pi/\delta$. The effects of higher frequencies are only visible within one time interval. Assuming constant references within a single interval $t \in [k\delta, (k+1)\delta]$ the effect of the reference using equation (8) is given by

$$\begin{aligned} z(k\delta) &= \bar{M} z(k\delta^-) + \bar{P} r(k\delta) \\ &= A_\mathrm{d} z((k-1)\delta) + \bar{P} r(k\delta) + \\ &\underbrace{\left(\bar{M}\int_0^\delta (\delta-\tau)^{\alpha-1}\mathcal{E}_{\alpha,\alpha}(F(\delta-\tau)^\alpha) B_\mathrm{cl}\mathrm{d}\tau\right)}_{\tilde{B}_\mathrm{d}} r((k-1)\delta). \end{aligned}$$

Matrix $\tilde{B}_\mathrm{d}$ can be simplified further using properties of the Mittag-Leffler function (Podlubny, 1999), that is

$$B_\mathrm{d} = \bar{M}\delta^\alpha \mathcal{E}_{\alpha,\alpha+1}(F\delta^\alpha) B_\mathrm{cl}. \tag{27}$$

Compared to simple memory reset the induced discrete dynamics show the additional term $\bar{P}r((k+1)\delta)$ in

$$z((k+1)\delta) = A_\mathrm{d} z(k\delta) + B_\mathrm{d} r(k\delta) + \bar{P} r((k+1)\delta). \tag{28}$$

Here the reference at the time instant δk directly influences the extended state at the same time instant. This extra term accelerates the induced discrete dynamics. In order to remove the time shift in representation (28) we consider the transformation

$$\gamma(k\delta) = z(k\delta) - \bar{P} r(k\delta). \tag{29}$$

With $\begin{pmatrix}\bar{C} & 0\end{pmatrix}\bar{P} = 0$ we have

$$\gamma((k+1)\delta) = A_\mathrm{d}\gamma(k\delta) + \left(A_\mathrm{d}\bar{P} + B_\mathrm{d}\right) r(k\delta) \tag{30}$$

$$y(k\delta) = \begin{pmatrix}\bar{C} & 0\end{pmatrix}\gamma(k\delta) + D_\mathrm{cl} r(k\delta). \tag{31}$$

For the low frequency range $\omega < \pi/\delta$ the frequency-response of the closed-loop is approximated by

$$T_\mathrm{low}(z) = \begin{pmatrix}\bar{C} & 0\end{pmatrix}(zI - A_\mathrm{d})^{-1}\left(A_\mathrm{d}\bar{P} + B_\mathrm{d}\right) + D_\mathrm{cl}. \tag{32}$$

This frequency domain interpretation can be used to tune the reset parameters $M_\mathrm{c}, N_\mathrm{c}$ and P_c. In order to achieve zero steady-state error the DC gain of (32) has to be one. The stationary control signal u_∞ is given by the baseline controller, assuming it is designed to let $e_{t\to\infty}(t) = 0$, thus

$$u_\infty = K_\mathrm{DC}\, r_\infty \quad \text{with} \quad K_\mathrm{DC} = \frac{C(0)}{1 + C(0)G(0)}. \tag{33}$$

We consider the discrete dynamics at a stationary point ${}_{k\delta}\mathcal{D}^\alpha x_\mathrm{c}(t) = 0$ with $e(t) = 0$ and wish that the control output is unchanged after the reset. With $e(t) = 0$ the control effort only depends on the control signal $u_\infty = C_\mathrm{c} x_{c,\infty}$. Hence we require for (21b) that

$$x_{c,\infty} = M_\mathrm{c} x_{c,\infty} + N_\mathrm{c} r_\infty. \tag{34}$$

There are various choices for M_c and N_c satisfying (34). In the spirit of Zheng et al. (2008) we propose

$$M_\mathrm{c} = \mu I \tag{35}$$

$$C_\mathrm{c} N_\mathrm{c} = (1-\mu) K_\mathrm{DC} \tag{36}$$

with $\mu \in [0, 1]$. Then

$$\begin{aligned} & (1-\mu) I x_{c,\infty} = N_\mathrm{c} x_{c,\infty} \\ \iff \quad & (1-\mu) C_\mathrm{c} x_{c,\infty} = C_\mathrm{c} N_\mathrm{c} r_\infty \\ \iff \quad & (1-\mu) K_\mathrm{DC} r_\infty = C_\mathrm{c} N_\mathrm{c} r_\infty. \end{aligned}$$

For $\mu = 1$ the stationary behavior is determined by the baseline controller such that its robustness properties are conserved by the reset. For $P_\mathrm{c} = 0$ this resembles the pure memory reset scheme. On the contrary, for $\mu = 0$ the reset controller state is completely given by the reference and gain K_DC. In this case, discrete time system matrix A_d has a rank of at least n. Thus, all dynamics added by the controller are removed by the reset ($M_\mathrm{c} = 0$). This leads to a fast closed-loop response, however, robustness properties of the baseline controller are removed. The remaining parameter P_c can be used to reduce the frequency peak of (32) induced by the memory-reset.

4. IMPLEMENTATION

In order to simulate or realize FO control, implementation of FO integrals is necessary. Direct implementation of the FO integral (1) has two main problems: First, the memory of typical implementation platforms is limited. So, either the short memory principle introduces an error or the operator is only applied on a fixed horizon. For the memory reset controller, this horizon is given by time interval δ. The second difficulty of a direct numerical integration is the singularity of the convolution kernel at the lower limit $t \to t_0$.

4.1 Implementation Using Higher-Order Approximations

It is common to use higher-order band-limited approximations, e.g. continuous fraction approximation (Monje et al., 2010) or the Oustaloup filter (Monje et al., 2010; Tepljakov et al., 2011). The Oustaloup filter is designed to mimic the FO operator in frequency band $\Omega = \{\omega \in \mathbb{R} | \omega_l \le \omega \le \omega_h\}$, and obeys

$$s^\alpha \approx H_\alpha(s) = \omega_h^\alpha \prod_{k=-N}^{N} \frac{s + \omega_k^-}{s + \omega_k^+} \tag{37}$$

with

$$\omega_k^\pm = \omega_l \left(\frac{\omega_h}{\omega_l}\right)^{\frac{k+N+(1\pm\alpha)/2}{2N+1}}. \tag{38}$$

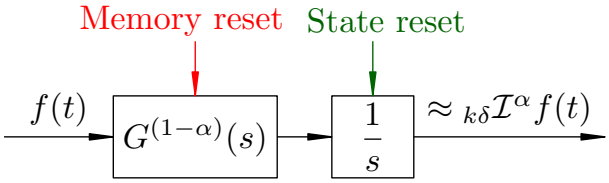

Fig. 2. This approximation splits the pseudo state from its memory (HosseinNia, 2013) .

While these approximations are useful, they may lead to stationary error. Consider a simple system of the form

$$G^*(s) = \frac{1}{s^\alpha + 1} \tag{39}$$

with the unity DC-gain $G^*(0) = 1$. Inserting the direct approximation (37), however, leads to a wrong DC gain:

$$\frac{1}{H_\alpha(0)+1} = \left(1 + \omega_h^\alpha \prod_{k=-N}^{N} \left(\frac{\omega_h}{\omega_l}\right)^{-\alpha/(2N+1)}\right)^{-1} = \frac{1}{1+\omega_l^\alpha} \neq G^*(0).$$

In the spirit of HosseinNia (2013) we use an additional integrator such that the new approximation of the FO integrator

$$s^{-\alpha} = \frac{s^{1-\alpha}}{s} \approx \frac{H_{1-\alpha}(s)}{s} \tag{40}$$

leads to a new approximation $\tilde{G}^*(s)$ with a correct DC-gain:

$$\tilde{G}^*(s)\Big|_{s=0} = \frac{H_{1-\alpha}(s)}{s + H_{1-\alpha}(s)}\Big|_{s=0} = 1. \tag{41}$$

This approach preserves the integration properties of the FO integrator for frequencies below the design bandwidth $\Omega = \{\omega \in \mathbb{R} | \omega_l \leq \omega \leq \omega_h\}$. The integer-order integrator can be associated with the actual (pseudo) state of the FO controller, the remaining part is an approximation of the memory introduced by the FO derivative. The initial conditions of the (pseudo) state x_c define in which order the integrator and the approximation $H_{1-\alpha}(s)$ have to be used. This is illustrated in Fig. 2, showing the differences of the reset strategies.

Each element of the pseudo state has its own past, therefore the implementation requires η additional systems:

$$\tilde{H}(s) = \mathrm{diag}\left(H_{1-\alpha}(s), \ldots, H_{1-\alpha}(s)\right) = \left[\begin{array}{c|c} \tilde{A} & \tilde{B} \\ \hline \tilde{C} & \tilde{D} \end{array}\right]$$

with the approximation order N, such that $\tilde{A} \in \mathbb{R}^{\eta N \times \eta N}$. Applying this approach to the FO controller (14a)-(14c) results in

$$\begin{pmatrix} \dot{x}_\mathrm{c}(t) \\ \dot{\tilde{x}}_\mathrm{c}(t) \end{pmatrix} = \underbrace{\begin{pmatrix} \tilde{D}A_\mathrm{c} & \tilde{C} \\ \tilde{B}A_\mathrm{c} & \tilde{A} \end{pmatrix}}_{\tilde{A}_\mathrm{c} \in \mathbb{R}^{\eta(N+1)\times\eta(N+1)}} \begin{pmatrix} x_\mathrm{c}(t) \\ \tilde{x}_\mathrm{c}(t) \end{pmatrix} + \underbrace{\begin{pmatrix} \tilde{D}B_\mathrm{c} \\ \tilde{B}B_\mathrm{c} \end{pmatrix}}_{\tilde{B}_\mathrm{c} \in \mathbb{R}^{\eta(N+1)\times q}} e(t) \tag{42a}$$

$$u(t) = \underbrace{\begin{pmatrix} C_\mathrm{c} & 0 \end{pmatrix}}_{\tilde{C}_\mathrm{c} \in \mathbb{R}^{p\times\eta(N+1)}} \begin{pmatrix} x_\mathrm{c}(t) \\ \tilde{x}_\mathrm{c}(t) \end{pmatrix} + \underbrace{D_\mathrm{c}}_{D_\mathrm{c} \in \mathbb{R}^{p\times q}} e(t) \tag{42b}$$

with the extended state $\begin{pmatrix} x_\mathrm{c}^\top & \tilde{x}_\mathrm{c}^\top \end{pmatrix}^\top$ containing the (pseudo) controller state x_c and its individual memory $\tilde{x}_\mathrm{c}$.

The direct approximation of the FO integral using equation (37) leads to a relative degree of zero. With the applied split of the FO integrator, the overall approximation is of relative degree one, which is important in order to avoid algebraic loops.

For system (6) with $\alpha = 1$ and the approximation (42) the closed-loop is given by

$$\dot{\zeta}(t) = \underbrace{\begin{pmatrix} A - BD_\mathrm{c}C & B\tilde{C}_\mathrm{c} \\ -\tilde{B}_\mathrm{c}C & \tilde{A}_\mathrm{c} \end{pmatrix}}_{\tilde{F}} \zeta(t) + \begin{pmatrix} BD_\mathrm{c} \\ \tilde{B}_\mathrm{c} \end{pmatrix} r(t)$$

$$y(t) = \begin{pmatrix} C - DD_\mathrm{c}C & D\tilde{C}_\mathrm{c} \end{pmatrix} \zeta(t) + (DD_\mathrm{c})\, r(t)$$

with

$$\zeta^\top = \begin{pmatrix} x^\top & x_\mathrm{c}^\top & \tilde{x}_\mathrm{c}^\top \end{pmatrix}^\top. \tag{43}$$

Note that this representation uses the approximation of the controller instead of the associated FO system.

Consider the general reset law (21b). At the reset instant $t = k\delta$ the extended state is determined by the reset matrix $\bar{M}$ according to

$$\zeta(k\delta) = \bar{M}\,\zeta(k\delta^-). \tag{44}$$

The differences of the controller approaches become evident when comparing the different state reset matrices. In case of a state reset the memory approximation $\tilde{x}_\mathrm{c}$ remains unchanged, that is

$$\tilde{M}_\mathrm{state} = \begin{pmatrix} I & 0 & 0 \\ -P_\mathrm{c}C & M_\mathrm{c} & 0 \\ 0 & 0 & I \end{pmatrix}. \tag{45}$$

In case of the memory and the extended memory reset the controller memory is set to zero, hence the last column is zero. So here we have

$$\tilde{M}_\mathrm{memory} = \begin{pmatrix} I & 0 & 0 \\ 0 & I & 0 \\ 0 & 0 & 0 \end{pmatrix}, \quad \tilde{M}_\mathrm{extended} = \begin{pmatrix} I & 0 & 0 \\ -P_\mathrm{c}C & M_\mathrm{c} & 0 \\ 0 & 0 & 0 \end{pmatrix}. \tag{46}$$

This approximation also can be used to examine stability of the implementation for the pure state reset controller.

Theorem 3. (Stability). The approximation of the fractional-order controller (42) with reset law (21b) stabilizes the origin of the system (6) with $\alpha = 1$ asymptotically iff

$$\left|\lambda_i\left(\tilde{M}_\mathrm{state} \exp\left(\tilde{F}\delta\right)\right)\right| < 1, \tag{47}$$

where $\lambda_i(\cdot)$, $i = 1, 2, \ldots, n + \eta + \eta N$, denotes the i-th eigenvalue of the induced discrete system matrix.

Proof. The induced discrete-time homogeneous dynamics including the approximation of the FO controller are

$$\zeta((k+1)\delta) = \tilde{M}_\mathrm{state} \exp\left(\tilde{F}\delta\right) \zeta(k\delta) = \tilde{A}_\mathrm{d}\zeta(k\delta). \tag{48}$$

If this control concept is applied to a FO process, we can expand this method to analyse the stability of the closed loop system. Thus we have to include an approximation of the memory of the FO system. The results, however, rely on the quality of the approximation and are not robust.

Similar to the FO cases before (see Section 3.1), we can extend the description of the induced dynamics by the effect of constant reference inputs to derive an approximation of the frequency response for the lower frequency range $\omega < \pi/\delta$ and obtain

$$\tilde{T}(z) = \tilde{C}_\mathrm{cl}\left(zI - \tilde{A}_\mathrm{d}\right)^{-1} \tilde{B}_\mathrm{d} + DD_\mathrm{c} \tag{49}$$

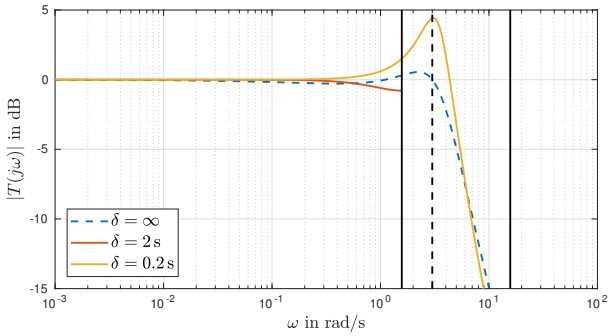

Fig. 3. Amplitude response of the baseline controller (dashed blue), and the memory reset controller for different initialization intervals.

with

$$\tilde{B}_\mathrm{d} = \tilde{M}_\mathrm{state} \int_0^\delta \exp(\tilde{F}(t-\tau))\mathrm{d}\tau \begin{pmatrix} BD_\mathrm{c} \\ \tilde{B}_\mathrm{c} \end{pmatrix} + \tilde{A}_\mathrm{d}\tilde{P}. \quad (50)$$

Remark A further generalized framework regarding the reset of the FO controller should include both aspects: resetting to arbitrary values the controller state and the memory. If striving to describe the memory exactly we have to use the distributed state representation by Sabatier et al. (2014), i.e.

$${}_{t_0}\mathcal{D}^\alpha f(t) = \int_0^\infty \frac{\sin(1-\alpha)}{\pi} \omega^{\alpha-1} \xi(\omega,t)\mathrm{d}\omega \quad (51)$$

with the evolution of the distributed state $\xi(\omega,t)$ given by

$$\dot{\xi}(\omega,t) = -\omega\xi(\omega,t) + \dot{f}(t). \quad (52)$$

4.2 Direct Implementation via Differentiation

We are now discussing the problem related to the singular convolution kernel. In (Brzeziski and Ostalczyk, 2014) a transformation of the integration variable τ is considered. Due to the fixed horizon of the controller this method is not suitable here. We propose a different approach by splitting the integral (1) via partial integration for $\alpha \in (0,1)$:

$${}_{t_0}\mathcal{I}^\alpha f(t) = \frac{1}{\Gamma(\alpha)} \left[\frac{t^\alpha}{\alpha} f(t_0) - \int_{t_0}^t \frac{\dot{f}(\tau)(t-\tau)^\alpha}{\alpha} \mathrm{d}\tau \right]. \quad (53)$$

For continuously differentiable functions $f(\cdot) \in \mathcal{C}^1$ the singularity in the integrand is removed and the remaining convolution with the kernel

$$\bar{Y}_\alpha(t) = \frac{t_+^\alpha}{\Gamma(\alpha+1)} = \begin{cases} \dfrac{t^\alpha}{\Gamma(\alpha+1)}, & t > 0 \\ 0, & t \le 0 \end{cases} \quad (54)$$

can be solved with standard methods like the trapezoidal rule. A drawback of the real-time implementation, however, is the need of a derivative. Except for the exact robust sliding-mode differentiator by Levant (2018), the derivative can only be implemented with an additional pole ("dirty derivative").

In order to avoid the differentiation of a possible noisy signal we shift the order of operations: Instead of solving the convolution $\bar{Y}_\alpha(t) \star \dot{f}(t)$, we solve the convolution with the function itself $\bar{Y}_\alpha(t) \star f(t)$ and differentiate the result. Applying Leibniz' rule we get

$$\begin{aligned} \frac{\mathrm{d}}{\mathrm{d}t}\left(\bar{Y}_\alpha(t) \star \dot{f}(t)\right) &= \frac{\mathrm{d}}{\mathrm{d}t}\left[\frac{1}{\Gamma(\alpha)} \int_0^t f(\tau)(t-\tau)^\alpha \mathrm{d}\tau\right] \\ &= \frac{1}{\Gamma(\alpha+1)} \int_0^t \frac{\mathrm{d}}{\mathrm{d}t}\left[f(\tau)(t-\tau)^\alpha\right]\mathrm{d}\tau \\ &= \frac{\alpha}{\Gamma(\alpha+1)} \int_0^t f(\tau)(t-\tau)^{\alpha-1}\mathrm{d}\tau = {}_0\mathcal{I}^\alpha f(t). \end{aligned}$$

In doing so we can exchange the order of operations and avoid the direct differentiation of a noisy measurement signal, e.g. the tracking error in the case of a FO integrator. Furthermore the result of this exchanged order is independent of the initial value of the function $f(0)$ which might also be effected by noise.

Now we are in the position to apply a proper differentiator

$$G_\mathrm{diff}(s) = \frac{s}{T_N s + 1} \quad (55)$$

to compute the FO integral. If the additional pole $T_N s+1$ decreases the closed-loop dynamics significantly, it can be considered in the controller design by devising the controller for the modified process

$$\tilde{G}(s) = \frac{G(s)}{T_N s + 1}. \quad (56)$$

The numerical evaluation of the convolution integral without singularity requires still the complete history of $f(t)$ within the time interval $t \in [0,\delta]$. Applying the trapezoidal rule, the online integration of the sampled function $f(kT_\mathrm{s})$ results in the multiplication of the history vector $H(kT_\mathrm{s}) \in \mathbb{R}^N$ and the sampled new kernel $K(kT_\mathrm{s}) \in \mathbb{R}^{1\times N}$ with $N = \delta/T_\mathrm{s} + 1$:

$$\int_0^t f(\tau)(t-\tau)^{\alpha-1}\mathrm{d}\tau\Big|_{t=kT_\mathrm{s}} \approx K(kT_\mathrm{s})\ H(kT_\mathrm{s})\ T_\mathrm{s} \quad (57)$$

with j-th element at the time instant $t = kT_\mathrm{s}$ defined as

$$H_j(kT_\mathrm{s}) = \begin{cases} f(jT_\mathrm{s}), & j \le k \\ 0, & j > k \end{cases}$$

$$K_j(kT_\mathrm{s}) = \begin{cases} \dfrac{1}{2}((j-k)T_\mathrm{s})^\alpha, & j = 1 \\ ((j-k)T_\mathrm{s})^\alpha, & j \le k \\ 0, & j > k \end{cases}$$

where the special weight for the first element $j = 1$ occurs due to the trapezoidal rule. Within this discrete-time framework we use a first-order Euler approximation

$$G_z(z) = \frac{z-1}{T_\mathrm{s} z} \quad (58)$$

to compute the derivative instead of (56). Within one reset period δ the counter k is limited to $k \in \{0,1,\ldots,N\}$.

Fig. 4 shows the results for a single interval. For comparison, different functions are integrated using the routine `fde12.m` by Diethelm and Freed (1999) with a much lower sampling time of 0.01 ms and an Oustaloup filter with different orders designed for the frequency range $\Omega = [10^{-3}\,\mathrm{rad\,s^{-1}}, 10^{3}\,\mathrm{rad\,s^{-1}}]$ with an additional integrator. The rather large error at the beginning of the interval is caused by the discrete differentiator and may be improved. Compared to high-order approximations, the proposed method leads to a reduced error at the end of the time interval. This is important for the memory reset control, as this final value is used to reinitialize the subsequent interval.

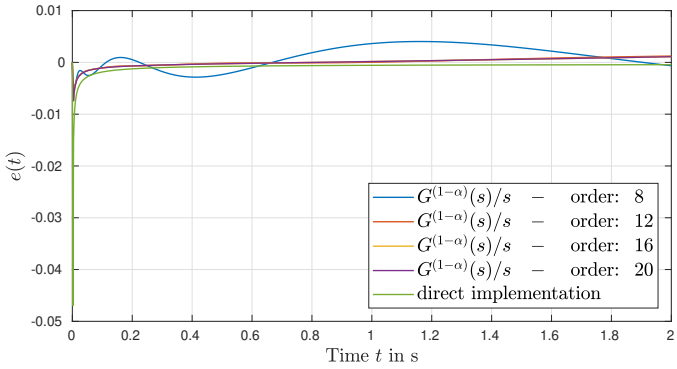

Fig. 4. Numerical error for sampling time $T_\mathrm{s} = 1\,\mathrm{ms}$, $f(t) = 1 + \sin(0.1t)$ and $\alpha = 0.4$.

5. SIMULATIONS AND EXPERIMENTAL RESULTS

We consider the velocity control of a DC motor. Its identified dynamics are given by

$$G(s) = \frac{K}{\tau s + 1} \quad \text{with} \quad K = 158.64,\ \tau = 0.8261. \tag{59}$$

The sampling time of the real-time interface is $T_\mathrm{s} = 2\,\mathrm{ms}$.

5.1 Simulation Results

The transfer function of the FO PI controller is given by

$$C_\mathrm{FOPI}(s) = K_\mathrm{P} + \frac{K_\mathrm{I}}{s^\alpha}. \tag{60}$$

The baseline controller is designed for crossover frequency of $\omega_\mathrm{c} = 3\,\mathrm{rad\,s^{-1}}$ and phase-margin of $\Phi_r = 60°$. The order $\alpha = \frac{2}{3}$ is chosen such the performance is acceptable with respect to overshooting. The design equations

$$|C(j\omega)G(j\omega)|_{\omega=\omega_\mathrm{c}} = 1$$
$$\pi + \arg(C(j\omega_\mathrm{c})G(j\omega_\mathrm{c}) = \frac{\pi}{3}$$

are solved using the standard non-linear routine `lsqnonlin` resulting in $K_\mathrm{P} = 0.0025$ and $K_\mathrm{I} = 0.0318$. For the implementation of the state reset controller we use an Oustaloup filter of the approximation order 19 with the frequency range $\Omega = [0.001\,\mathrm{rad\,s^{-1}}, 100\,\mathrm{rad\,s^{-1}}]$.

The closed-loop step responses with baseline controller as well as with various reset controllers using $\delta = 0.5\,\mathrm{s}$ is shown in Fig. 5. For comparison, a classical PI controller with the same crossover frequency is included. The algebraic convergence of the FO baseline controller is clearly visible for $t > 3\,\mathrm{s}$ (yellow line). The pure memory reset control (purple line) achieves exponential convergence, however the overshoot increases significantly. This corresponds to the peak of frequency response of the induced discrete dynamics as indicated in Fig. 3.

The reset parameters for the state and extended memory reset controller are chosen according to (35), (36) with $\mu = 0.1$ and $P_\mathrm{c} = 0$, resulting in $M_\mathrm{c} = \frac{1}{10}, N_\mathrm{c} = \frac{9}{10K}$. The FO state-reset controller does not improve the convergence (see. Fig. 5, green line). The discrete-dynamics including the approximation (42) of the baseline controller exhibit a DC-gain different from one. The overshoot is reduced compared to the baseline controller. The extended memory reset controller achieves exponential convergence (see Fig. 5, cyan line) and does not increase the overshoot.

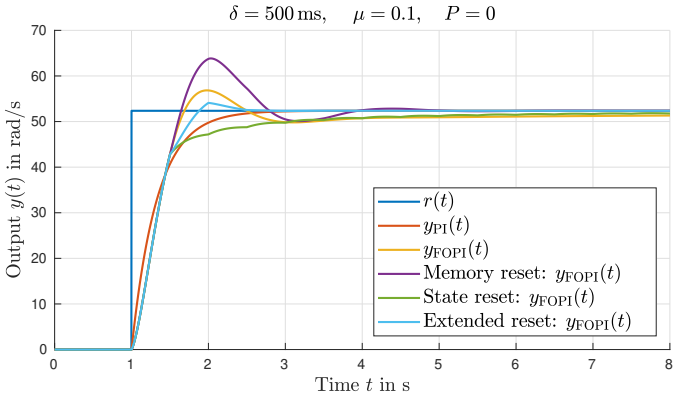

Fig. 5. Step reponses of different reset controllers.

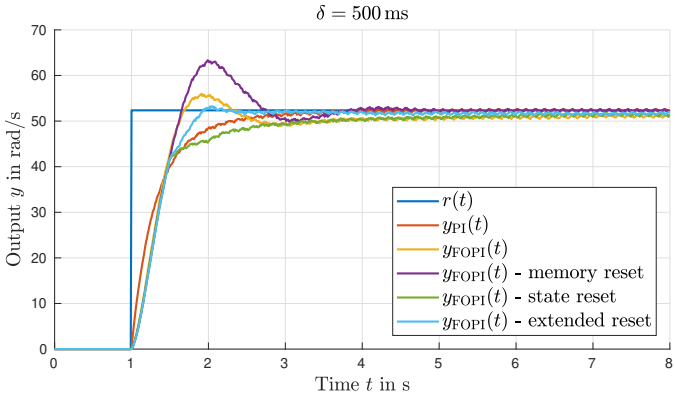

Fig. 6. Experimental results.

Note, that the analysis in Section 3.1 is based on a controller of order $\alpha^{-1} \in \mathbb{N}$. In order to map the design to this framework we need to consider an associated baseline controller of order $\bar{\alpha} = \frac{1}{3}$ and extended state-space. Accordingly, the reset maps $N_\mathrm{c}, M_\mathrm{c}, P_\mathrm{c}$ are adjusted in dimension and offer an increased degree of freedom. In this implementation we did not explore this additional degree of freedom due to memory limitations.

5.2 Experimental Validation

For the experimental verification, all controllers are applied to a DC-Motor driving an inertia and an eddy current brake. The velocity is obtained by differentiating the signal of an encoder signal applying (58).

It turns out that the stationary gain of the process deviates slightly from the identified data (59). Therefore the controller parameters are adapted to $K_\mathrm{P} = 0.0024, K_\mathrm{I} = 0.0312, M_\mathrm{c} = 0, N_\mathrm{c} = 0.0073$ and $P_\mathrm{c} = 0$. The results are shown in Fig. 6. For visibility the signals are down-sampled by averaging 5 samples. Overall the experiment confirms the simulation results. The ripples overlaying the steady state behavior correspond to the set speed of the system and thus is caused most likely by some imbalance of the rotating mass. The respective control signals are depicted in Fig. 7. Note that the stationary control effort differs from the model. All FO controllers exhibit a smaller peak in the control signal compared to the PI controller, while the memory and extended reset implementations also show exponential conversion. Moreover, the extended reset also reduces the overshoot significantly.

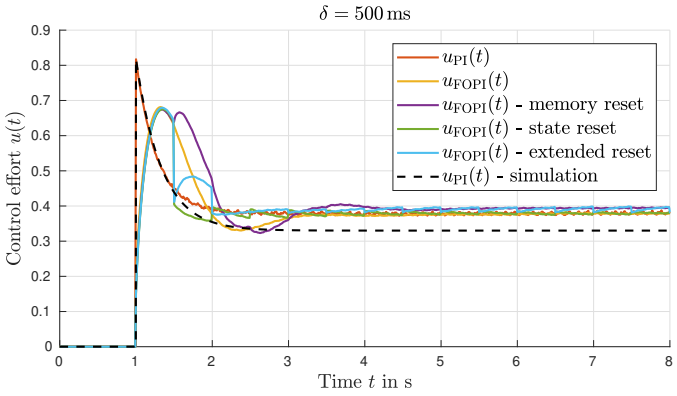

Fig. 7. Experimental control effort.

6. CONCLUSIONS

We expand a FO memory reset controller by the periodical resetting of the controller state. The amplitude response of the induced discrete system is used to tune the reset interval and the additional reset parameters. If including the reference for weighting the controller state reset, the stationary gain of the closed loop system must be known. Otherwise, the controller will lead to a stationary error.

Furthermoe, we propose a new implementation for the FO memory reset controller so as to enhance real-time capability and compare it to standard implementations. Differences to existing approaches are analysed by the approximative implementation. With this approach it is also possible to analyse the frequency behaviour of FO reset controllers without memory reset. Finally, the performance of all controllers is evaluated in simulation and experiment.

ACKNOWLEDGEMENTS

The first author gratefully acknowledges support by Deutsche Forschungsgemeinschaft (DFG) in the framework of the Research Training Group "Tip- and laser-based 3D-Nanofabrication in extended macroscopic working areas" (GRK 2182) at Technische Universität Ilmenau, Germany. The first and the third author acknowledge financial support from European Union Horizon 2020 research and innovation program, Marie Skłodowska-Curie grant agreement No. 824046.

REFERENCES

Brzeziski, D. and Ostalczyk, P. (2014). High-accuracy numerical integration methods for fractional order derivatives and integrals computations. *The Bulletin of the Polish Academy of Sciences: Technical Sciences*, 62(4), 723–733.

Diethelm, K. and Freed, A.D. (1999). The FracPECE subroutine for the numerical solution of differential equations of fractional order. *Forschung und wissenschaftliches Rechnen 1998*, 57–71.

HosseinNia, S.H., Tejado, I., and Vinagre, B.M. (2014a). Hybrid systems and control with fractional dynamics (II): Control. In *International Conference on Fractional Differentiation and its Applications*, 245–250.

HosseinNia, S.H., Tejado, I., Torres, D., Vinagre, B.M., and Feliu, V. (2014b). A General Form for Reset Control Including Fractional Order Dynamics. In *IFAC World Congress*, 2028–2033.

HosseinNia, S.H., Tejado, I., and Vinagre, B.M. (2013). Fractional-order reset control: Application to a servomotor. *Mechatronics*, 23(7), 781–788.

HosseinNia, S.H. (2013). *Fractional Hybrid Control Systems: Modeling, Analysis and Applications to Mobile Robotics and Mechatronics*. Ph.D. thesis, Universidad de Extremadura, Spain.

Levant, A. (2018). Filtering Differentiators and Observers. In *15th International Workshop on Variable Structure Systems*, 174–179.

Lorenzo, C.F. and Hartley, T.T. (2001). Initialization in fractional order systems. In *European Control Conference*, 1471–1476.

Matignon, D. (1996). Stability results for fractional differential equations with applications to control processing. In *Multiconference on Computational Engineering in Systems Applications*, 963–968.

Monje, C., Chen, Y., Vinagre, B., Xue, D., and Feliu-Batlle, V. (2010). *Fractional-order Systems and Controls: Fundamentals and Applications*. Springer.

Nesić, D., Teel, A.R., and Zaccarian, L. (2011). Stability and Performance of SISO Control Systems With First-Order Reset Elements. *IEEE Transactions on Automatic Control*, 56(11), 2567–2582.

Podlubny, I. (1999). *Fractional Differential Equations: An Introduction to Fractional Derivatives, Fractional Differential Equations, to Methods of Their Solution and Some of Their Applications*. Acad. Press.

Rugh, W.J. (1996). *Linear System Theory*. Prentice-Hall.

Sabatier, J., Farges, C., and Trigeassou, J.C. (2014). Fractional systems state space description: some wrong ideas and proposed solutions. *Journal of Vibration and Control*, 20(7), 1076–1084.

Sabatier, J., Moze, M., and Farges, C. (2010). LMI stability conditions for fractional order systems. *Computers & Mathematics with Applications*, 59(5), 1594–1609.

Tepljakov, A., Petlenkov, E., and Belikov, J. (2011). Fomcon: Fractional-order modeling and control toolbox for matlab. In *18th International Conference on Mixed Design of Integrated Circuits and Systems*, 684–689.

Weise, C., Wulff, K., and Reger, J. (2016). Exponentially Converging Observer for a Class of FO-LTI Systems. In *Multi-Conference on Systems and Control*, 723–729.

Weise, C., Wulff, K., and Reger, J. (2017). Fractional-order observer for integer-order LTI systems. In *Asian Control Conference*, 2101–2106.

Weise, C., Wulff, K., and Reger, J. (2019). Fractional-order memory reset control for integer-order LTI systems. In *Conference on Decision and Control*, 5710–5715.

Zheng, J., Guo, Y., Fu, M., Wang, Y., and Xie, L. (2008). Development of an extended reset controller and its experimental demonstration. *IET Control Theory Applications*, 2(10), 866–874.